



Supplement of

Multiscale modeling for coastal cities: addressing climate change impacts on flood events at urban-scale

Michele Bendoni et al.

Correspondence to: Carlo Brandini (brandini@lamma.toscana.it)

The copyright of individual parts of the supplement might differ from the article licence.

S1 Flooded Areas

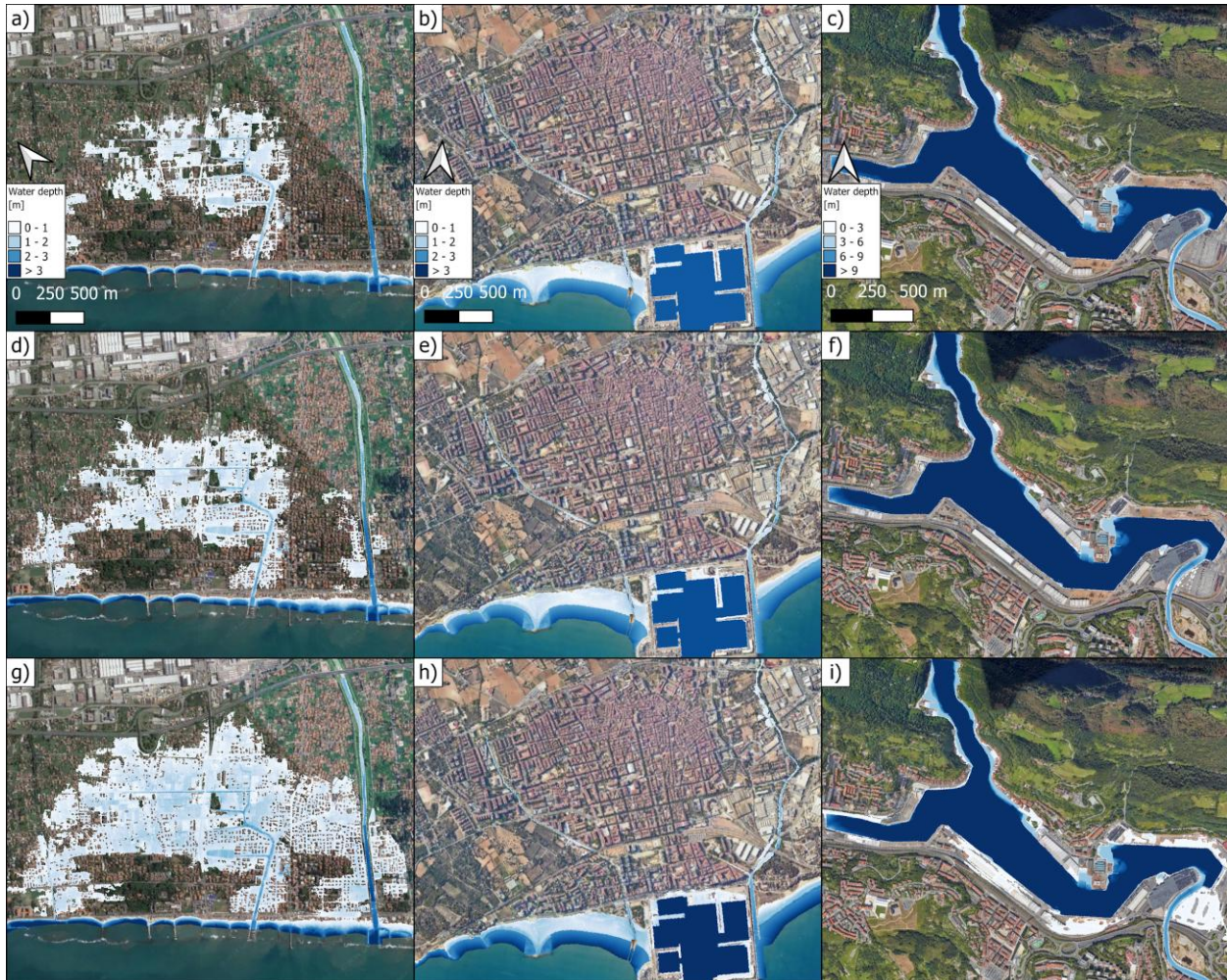


Fig S1 Hazard maps associated to the 100 years return period coastal flood event for the city of Massa: Historical a), RCP4.5 2011-2060 d), RCP8.5 2051-2100 g); for the city of Vilanova: Historical b), RCP4.5 2011-2060 e), RCP8.5 2051-2100 h); for the city of Oarsoaldea: Historical c), RCP4.5 2011-2060 f), RCP8.5 2051-2100 i). Maps data: © Google Earth 2024; images: © CNES / Airbus, Maxar Technologies, Airbus.



Fig S2 Hazard maps associated to the 100 years return period riverine flood event for the city of Massa: Historical a), RCP4.5 2011-2060 d), RCP8.5 2051-2100 g); for the city of Vilanova: Historical b), RCP4.5 2011-2060 e), RCP8.5 2051-2100 h); for the city of Oarsoaldea: Historical c), RCP4.5 2011-2060 f), RCP8.5 2051-2100 i). Maps data: © Google Earth 2024; images: © CNES / Airbus, Maxar Technologies, Airbus.

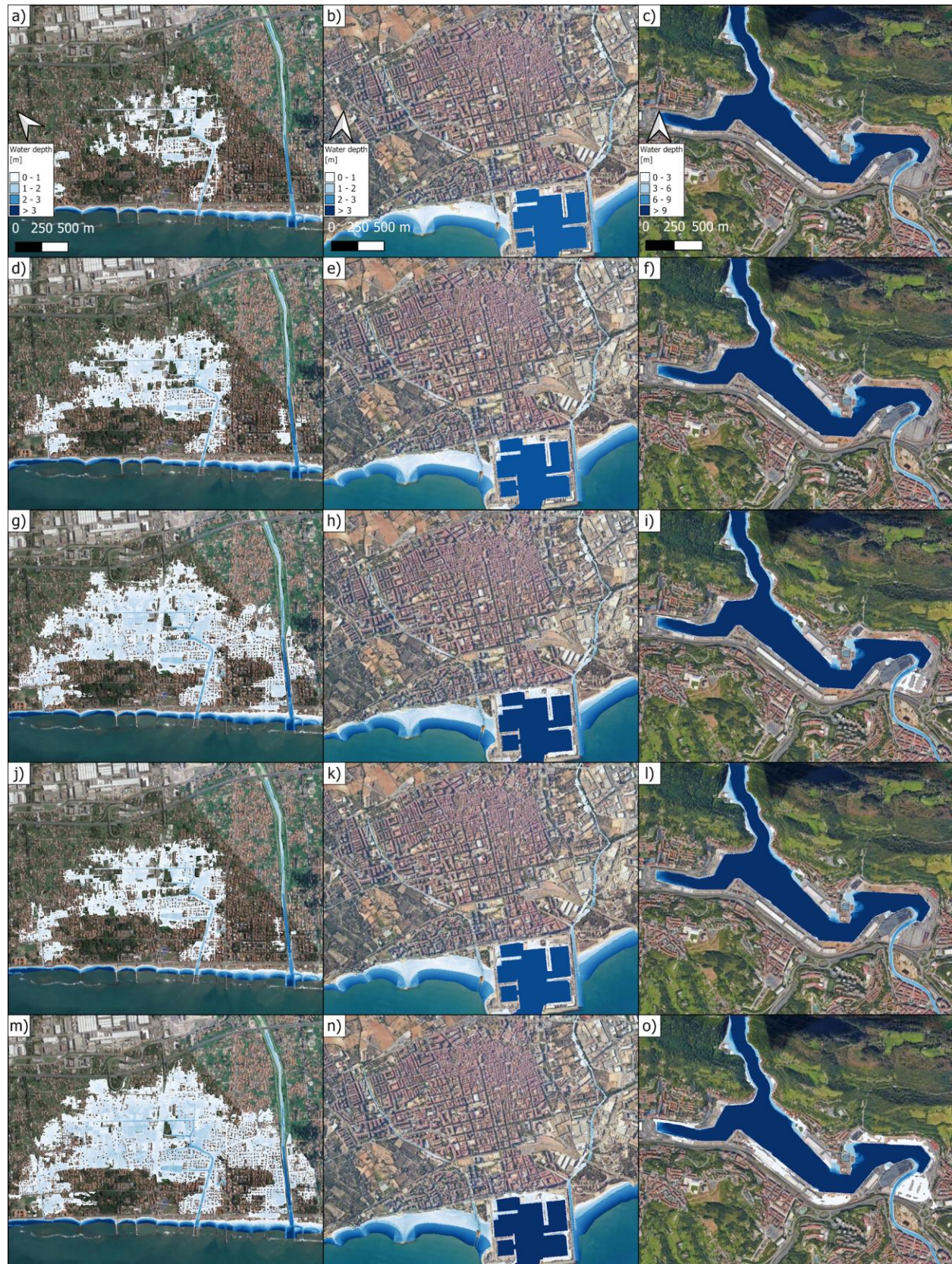


Fig S3 Hazard maps associated to the 25 years return period coastal flood event for the city of Massa: Historical a), RCP4.5 2011-2050 d), RCP4.5 2051-2100 g), RCP8.5 2011-2060 j), RCP8.5 2051-2100 m); for the city of Vilanova: Historical b), RCP4.5 2011-2050 e), RCP4.5 2051-2100 h), RCP8.5 2011-2060 k), RCP8.5 2051-2100 n); for the city of Oarsoaldea: Historical c), RCP4.5 2011-2050 f), RCP4.5 2051-2100 i), RCP8.5 2011-2060 l), RCP8.5 2051-2100 o). Maps data: © Google Earth 2024; images: © CNES / Airbus, Maxar Technologies, Airbus.

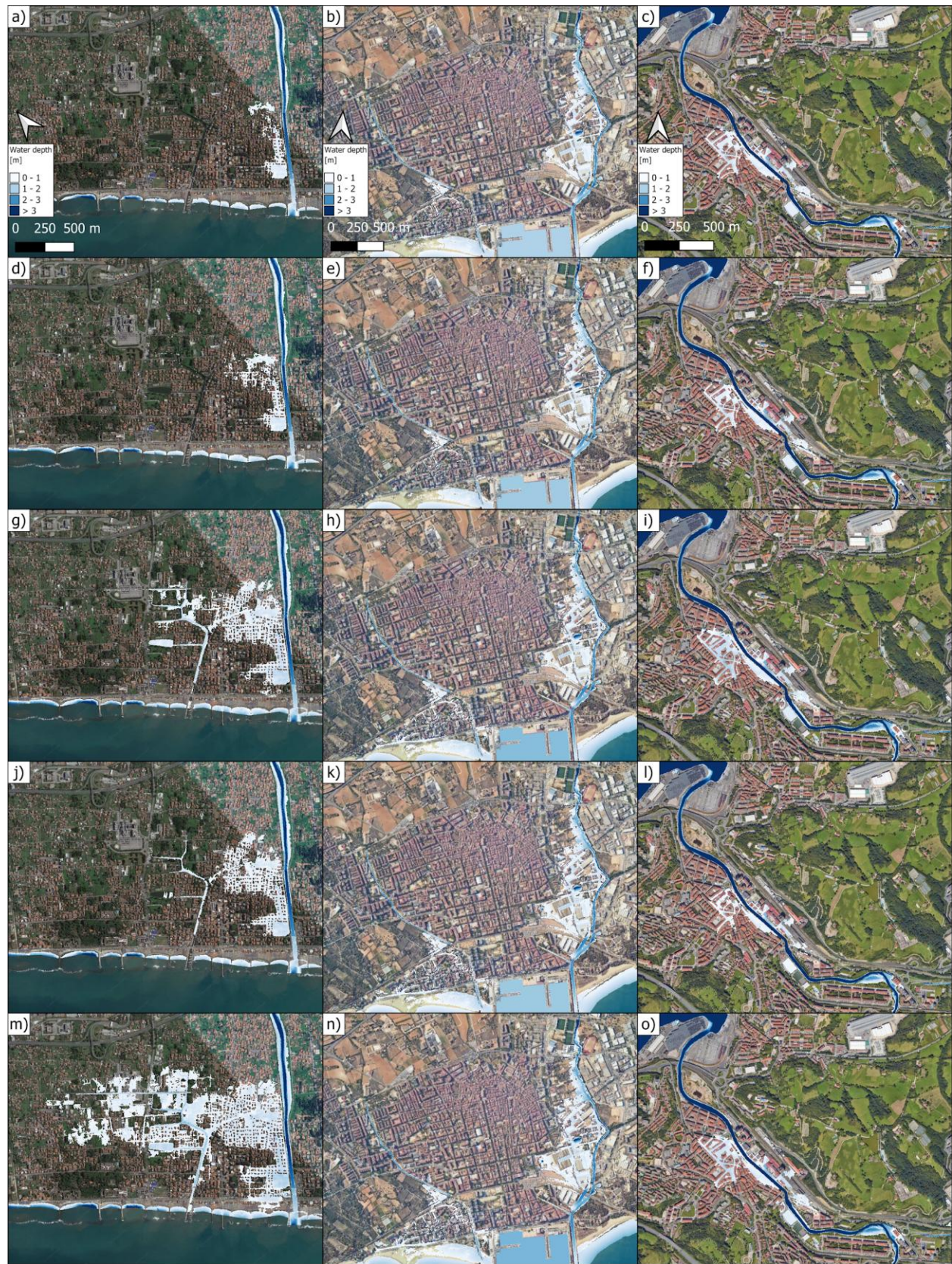


Fig S4 Hazard maps associated to the 25 years return period riverine flood event for the city of Massa: Historical a), RCP4.5 2011-2050 d), RCP4.5 2051-2100 g), RCP8.5 2011-2060 j), RCP8.5 2051-2100 m); for the city of Vilanova: Historical b), RCP4.5 2011-2050 e), RCP4.5 2051-2100 h), RCP8.5 2011-2060 k), RCP8.5 2051-2100 n); for the city of Oarsoaldea: Historical c), RCP4.5 2011-2050 f), RCP4.5 2051-2100 i), RCP8.5 2011-2060 l), RCP8.5 2051-2100 o). Maps data: © Google Earth 2024; images: © CNES / Airbus, Maxar Technologies, Airbus.

S2 Creation of boundary conditions

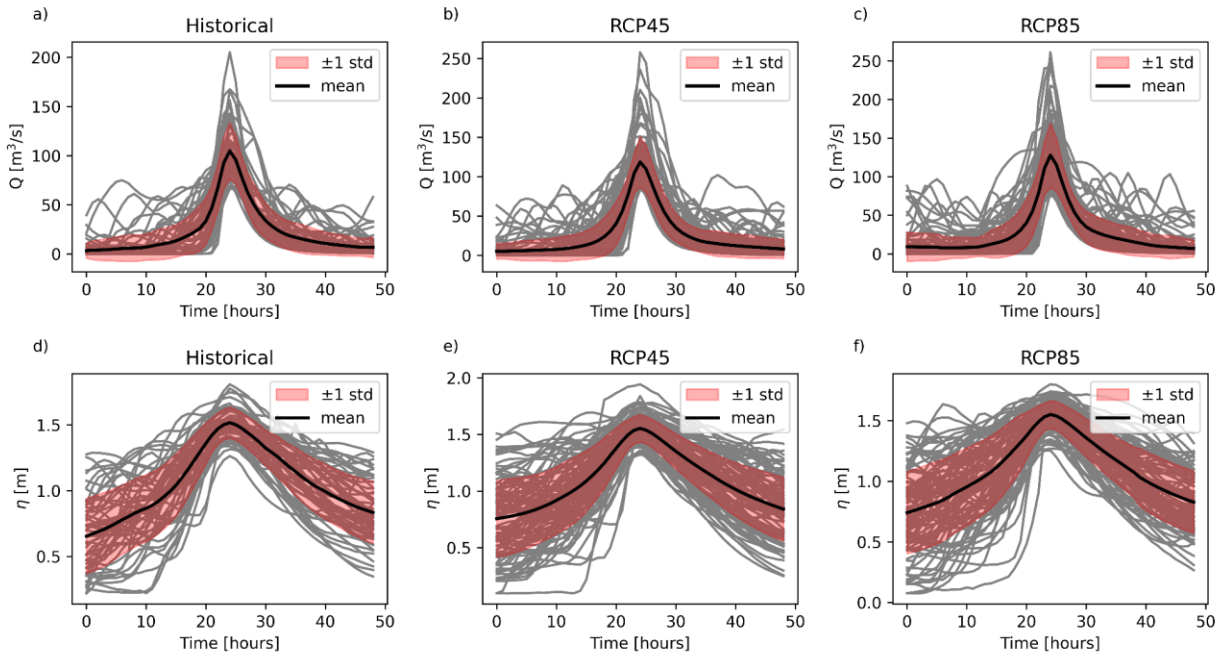


Fig S5 Shape of the synthetic hydrograph for the city of Massa. Centered yearly maximum time series are reported in grey, average in black, and ± 1 standard deviation is reported as shaded area. a), b), c) refer to discharge for Historical, RCP45 and RCP85 runs, respectively. d), e), f) refer to total water level for Historical, RCP45 and RCP85 runs, respectively.

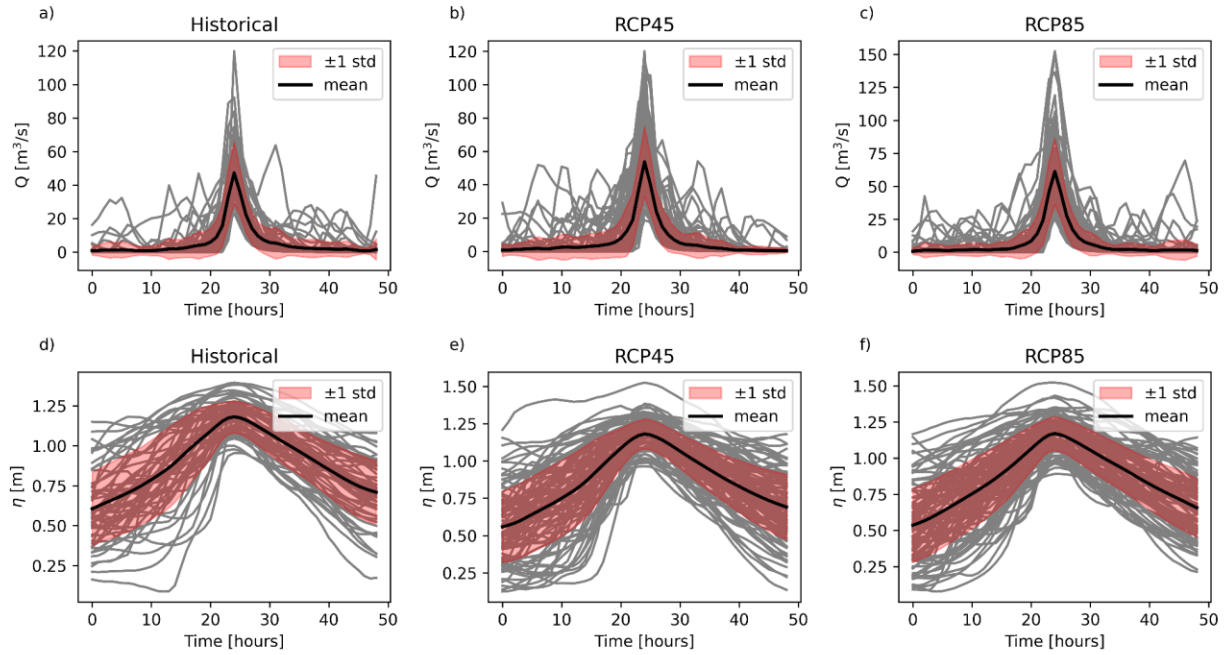


Fig S6 Shape of the synthetic hydrograph for the city of Villanova. Centered yearly maximum time series are reported in grey, average in black, and ± 1 standard deviation is reported as shaded area. a), b), c) refer to discharge for Historical, RCP45 and RCP85 runs, respectively. d), e), f) refer to total water level for Historical, RCP45 and RCP85 runs, respectively.

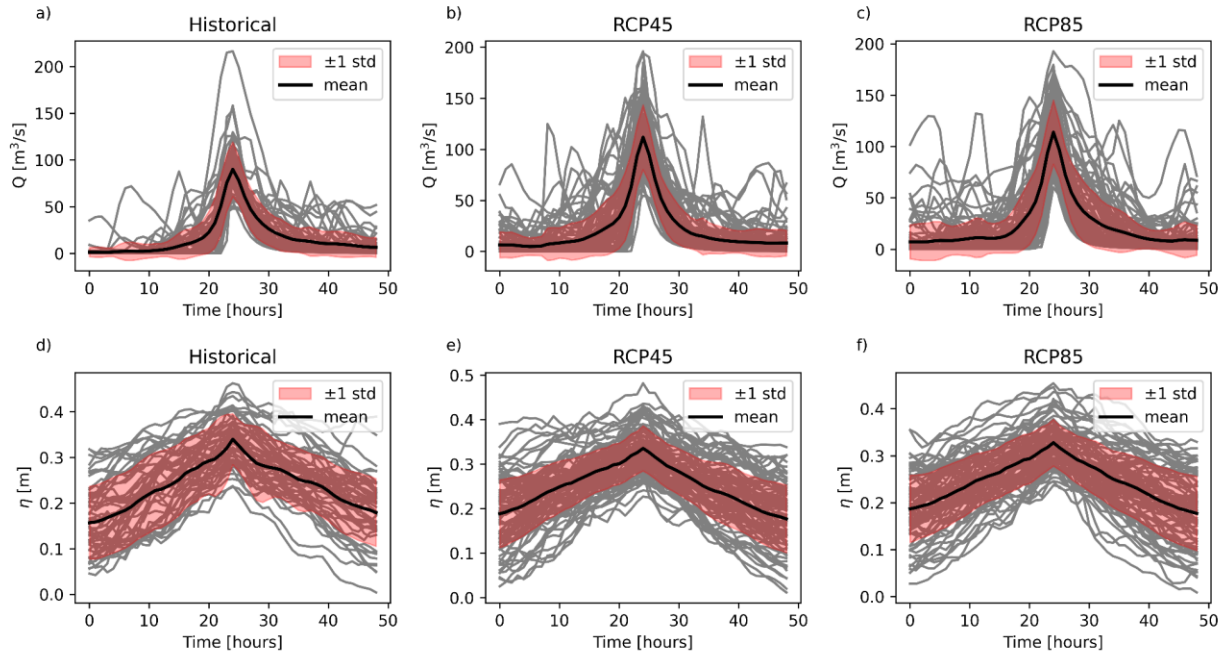


Fig S7 Shape of the synthetic hydrograph for the city of Oarsoaldea. Centered yearly maximum time series are reported in grey, average in black, and ± 1 standard deviation is reported as shaded area. a), b), c) refer to discharge for Historical, RCP45 and RCP85 runs, respectively. d), e), f) refer to water level for Historical, RCP45 and RCP85 runs, respectively.

S3 Calibration/validation procedure for the employed models

S3.1 Water level model (SHYFEM)

The water level model was calibrated and validated against observed data close to the city of Massa and Villanova, in the Mediterranean Sea, and Oarsoaldea, in the Atlantic Ocean. A trial and error procedure was used to identify the combination of wind drag and bottom friction coefficients leading to the best representation of the residual η (that is when the tidal components are removed). Modelled η values were compared to tidal gauge observations for the year 2012 for the city of Massa, and for the year 2020 for the city of Oarsoaldea. Wind and atmospheric pressure data at 3-hourly frequency from the Integrated Forecasting System (IFS) of the European Centre for Medium Range Weather Forecast (ECMWF) were used as atmospheric forcing for the calibration runs.

Model skill was estimated computing the correlation coefficient (CORR), the root mean squared error (RMSE) and BIAS for the whole time series and for η values higher than 0.25 m for Oarsoaldea and higher than 0.15 m for Massa roughly indicating moderate storm surge events (Marcos et al., 2011).

Several calibration runs were performed for the city of Oarsoaldea (tidal gauge located at Lon = -1.931 E; Lat = 43.321 N) with the best result given by: CORR = 0.81, RMSE = 0.08 m, BIAS = -0.06 m for the whole time series; RMSE = 0.09 m; BIAS = -0.01 for $\eta > 0.25$ m. Figure S8a and b presents the observed and modelled residual η from 9 calibration runs (m1 to m9), focusing on periods with residual water levels peaks reaching up to 47 cm. Despite the moderate variability in the computed values, most time series satisfactorily reproduce the observed signal, particularly during peak events. Results from simulations m8 correspond to the best calibration run.

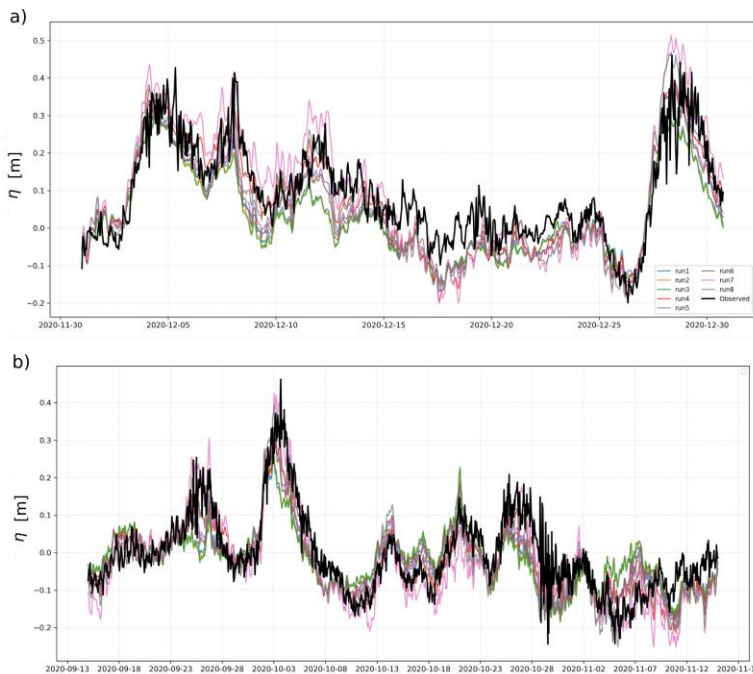


Fig S8 a) Time evolution of the observed and modelled residual water level for 9 calibration runs for December 2020 for the Oarsoaldea tidal gauge. b) Time evolution of the observed and modelled residual water level for 9 calibration runs from mid-September to mid November 2020 for the Oarsoaldea tidal gauge.

Same approach was employed for the city of Massa (tidal gauge located at Lon = 9.8576 E; Lat = 44.0966 N) for which the best calibration run gave the following results: CORR = 0.79, RMSE = 0.05 m, BIAS = 0.01 m for the whole time series; RMSE = 0.06 m, BIAS = 0.04 for $\eta > 0.15$ m. Figure S9a and b show the observed and modelled residuals for 9 calibration runs (m1 to m9). mX corresponds to the best calibration run.

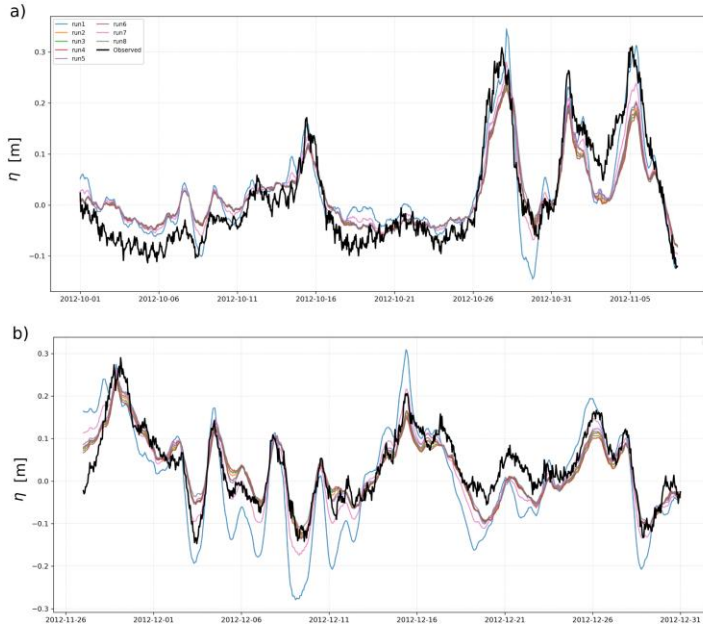


Fig S9 a) Time evolution of the observed and modelled residual water level for 9 calibration runs for October and a few days of November 2012 for the Massa tidal gauge. b) Time evolution of the observed and modelled residual water level for 9 calibration runs for the last part of November and December 2012 for the Massa tidal gauge.

Even for the other Mediterranean city, Villanova, the same procedure has been followed, obtaining similar estimation of the model prediction accuracy.

S3.2 Wave climate model (WWIII)

The wave model employed was already calibrated and validated by Vannucchi et al. (2021), but for a numerical mesh including only the Mediterranean Sea and different forcing fields based on a dynamic downscaling of the ERA-5 dataset (Hersbach et al., 2020). In the present work, the same calibrated parameters were adopted under the assumption that they remain valid outside the Mediterranean region as well.

For the present study, we report the model skill in reproducing the H_s with respect to observations from the Gorgona buoy (Lon = 9.96 E; Lat = 43.57 N), located in the Mediterranean Sea in the Tuscany Archipelago, and for one located close to Oarsoaldea, in the Atlantic Ocean (Lon = 1.89 E; Lat = 43.37 N). Even if the wave climate is not employed to simulate floods in Oarsoaldea, we report it for completeness of information.

For the Gorgona buoy, considering a period from 2009 to 2018, we obtained the following values: CORR = 0.64, RMSE = 0.65 m, BIAS = -0.11 m. Furthermore, to better quantify the model skill with respect to

the observed quantity, the standard deviation (STD) is equal to 0.77 m and maximum H_s ranging between 5 m and almost 8 m. In addition, we report the statistics obtained by Vannucchi et al. (2021) comparing the modelled values against the same buoy data: CORR = 0.92 RMSE = 0.29 m BIAS = -0.09 m. In Figure S10a and b, the time evolution of the observed and modelled H_s for the Gorgona buoy, for two periods characterized by intense wave climate, is reported.

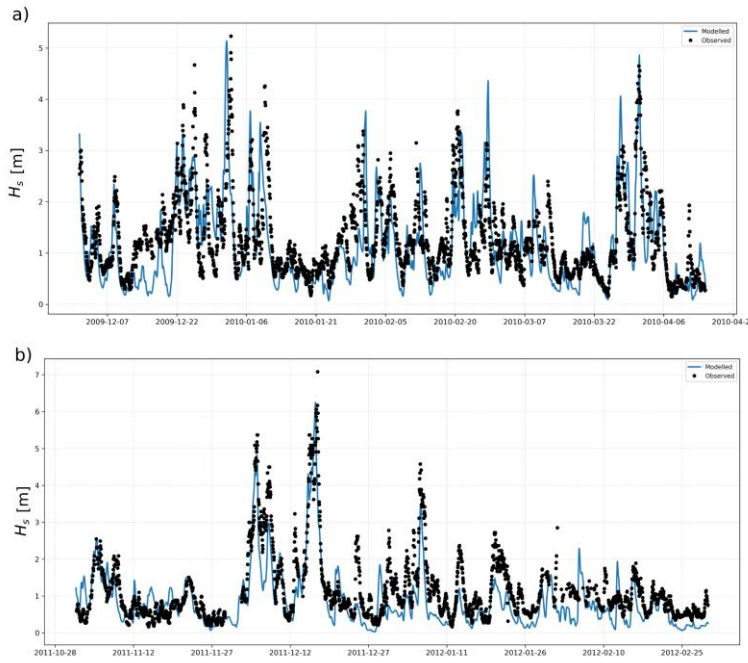


Fig S10 Time evolution of the observed and modelled significant wave height for the Gorgona buoy for two periods: a) from December 2009 to April 2010; b) from November 2011 to February 2012.

For the Oarsoaldea buoy, we have data from 2010 to 2012, and the model skill is summarized by the following values: CORR = 0.84, RMSE = 0.51 m, BIAS = -0.10 m, STD = 0.85 m. Maximum values range between 5 m and 8 m. Figures S11a and b, report the result for the Oarsoaldea buoy.

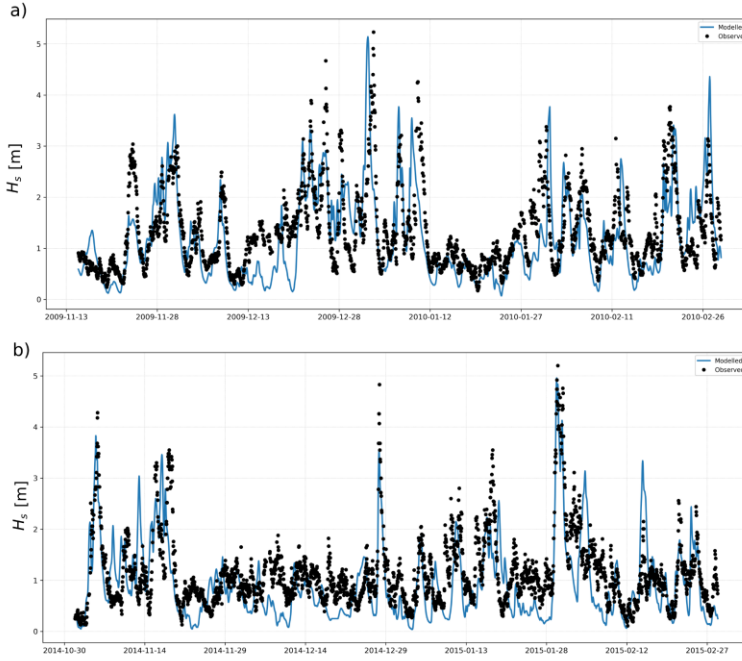


Fig S11 Time evolution of the observed and modelled significant wave height for the Oarsoaldea buoy for two periods: a) from November 2009 to February 2010; b) from November 2014 to February 2015.

Furthermore, Figure S12a and b report the QQ-plots for the observed (x-axis) and modelled (y-axis) H_s for the Gorgona and Oarsoaldea buoy, respectively. In both cases it is shown that the model tends to underestimate the largest wave heights.

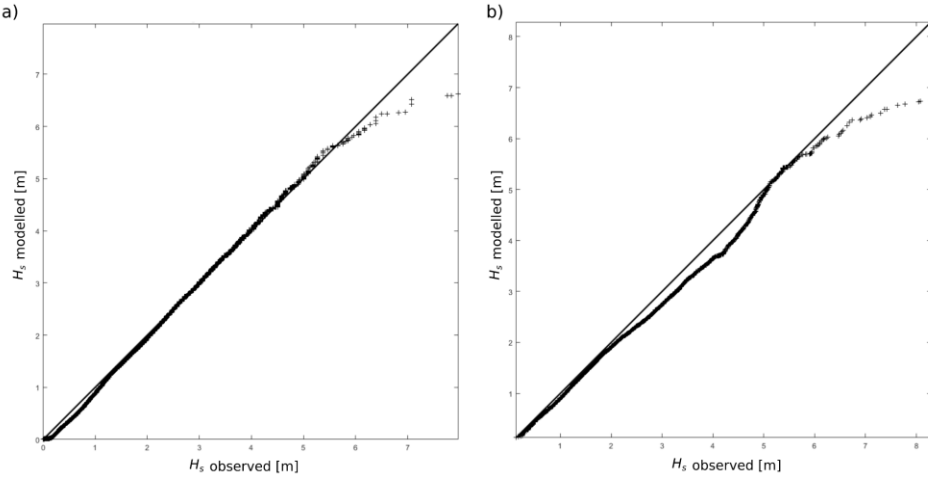


Fig S12 QQ-plots of the observed and modelled significant wave height for the Gorgona buoy a) and Oarsoaldea buoy b).

S3.3 Hydrological model (LISFLOOD)

LISFLOOD hydrological model was implemented for the three study areas (Massa, Villanova and Oarsoaldea) with a set of standard parameters selected within the values suggested from the routine calibration activities executed in the framework of the European Flood Awareness System (EFAS) for European basins, or worldwide for the Global Flood Awareness System (GloFAS). Both systems use

LISFLOOD in the operational modelling chain for flood hazard forecast (Ziese et al., 2019, Hirpa et al 2018, Dottori et al., 2022).

For the present application the main calibration parameters, i.e. the ones that control the infiltration capacity and runoff generation were set to $b_{\text{Xinjiang}} = 0.7$ and $\text{power_pre flow} = 3.5$. In order to evaluate the performance of the model with this configuration a set of focused simulations were performed on the Frigido river basin, where a water level gauge is present at the station of Canevara (located in the upper part of the basin, with a total catchment area of approx. 50 km^2). The simulation period goes from 2018 to 2021, when a valid stage-discharge relationship is available. Hourly precipitation time series required as meteorological forcing were retrieved from two ground-based gauges located in the upstream basin. Both water levels and precipitation data were provided by Tuscany Region Hydrological Service, www.sir.toscana.it). The other meteorological variables required for the LISVAP preprocessing step (incoming solar radiation, air temperature, dewpoint temperature, wind speed) were extracted from ERA5-Land product (Muñoz Sabater, J., 2019). An outlet point was added in LISFLOOD settings corresponding to the hydrometric gauge site and the hourly discharge time series obtained from the simulations were compared with the observed values.

Figure S13 shows the modelled and observed hydrographs for several events in the simulated period. The results show that the LISFLOOD model is in most cases capable of representing the flood peaks with adequate accuracy, whereas a general underestimation of baseflow and a steeper descendant limb of the hydrograph result from the model compared to the observed values. A more accurate baseflow estimation can be obtained with an improved groundwater representation and further calibration of the slow-response parameters. For the scope of the present study, that is focused on extreme events, the fair simulation of peak discharges was considered satisfactory, also considering the uncertainties related to spatial precipitation patterns and the relatively scarce data available in small basins.

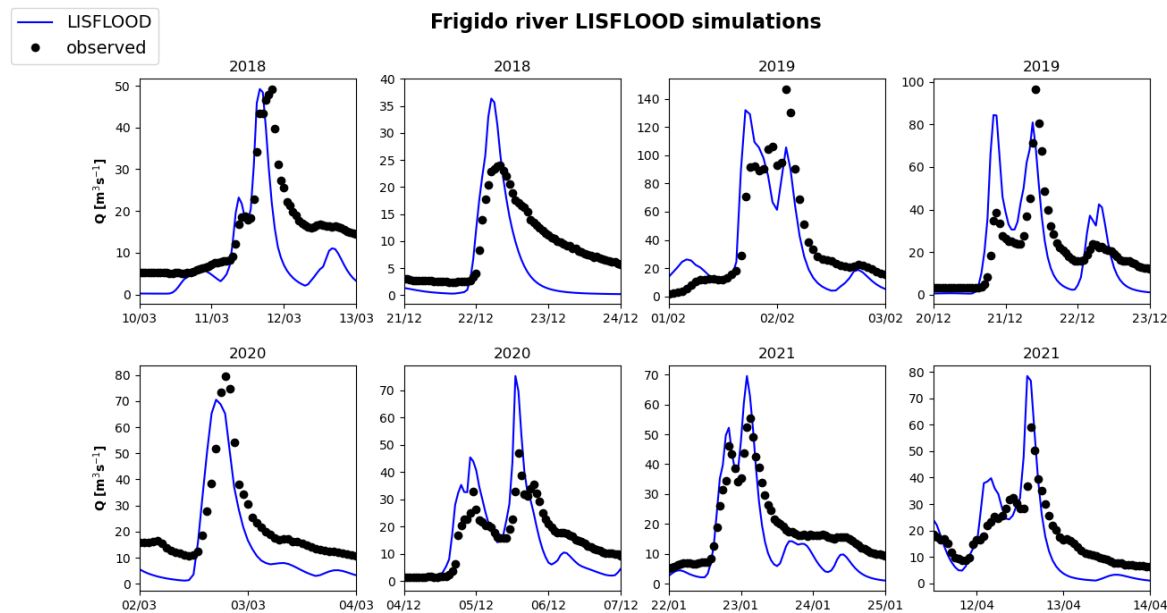


Fig S13 Modelled (blue line) and observed (black dots) hourly discharge for several events in the period 2018-2021 at Canevara hydrometric station on the Frigido river.

These simulations, performed using in-situ rainfall observations, confirm the capabilities of the LISFLOOD model to adequately reproduce the hydrological processes in the study basin. However, it is necessary to point out that, when the model is applied with different types of forcing, as in the case of global or regional climate models, additional uncertainties, biases and sources of errors may arise and clearly affect the accuracy of the hydrologic simulation. For example, we expect an underestimation of peak rainfall intensities when using gridded data with coarse spatial and temporal resolution.

Since the present work is dedicated to the general presentation of the modelling chain and the relative comparison between different climatologic scenarios, we did not address these aspects in detail but they are the object of further ongoing activities.

S4 Cumulative time persistence and events per year over a threshold

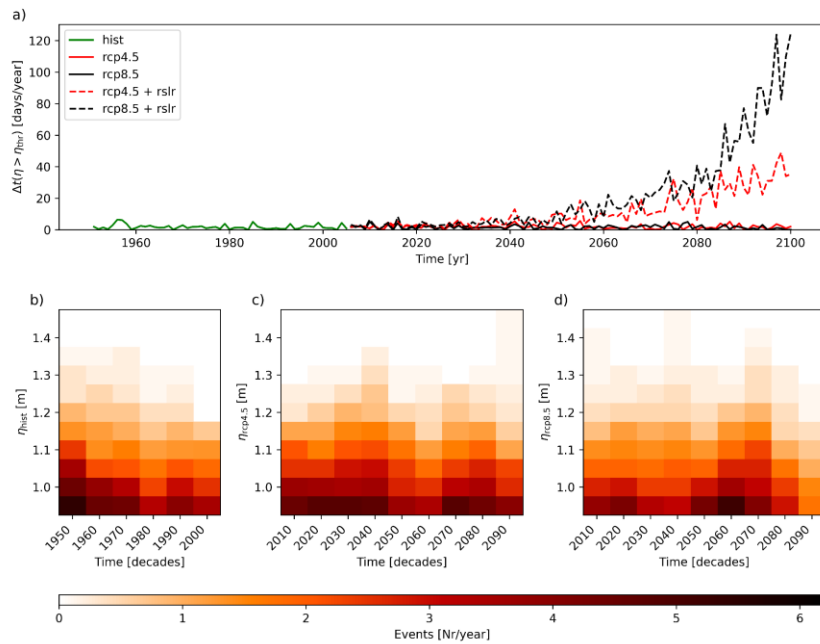


Fig S14 a) Cumulative duration of total water level above the 99.5 % -ile in days per year for HIST (green line), RCP4.5 (red line), RCP8.5 (black line), RCP4.5 and RCP8.5 plus the effect of RSLR (red dashed line and black dashed line, respectively), for the city of Villanova. Number of events per year with peak values larger than specific values, grouped by decades for: HIST b), RCP4.5 c) and RCP8.5 d)

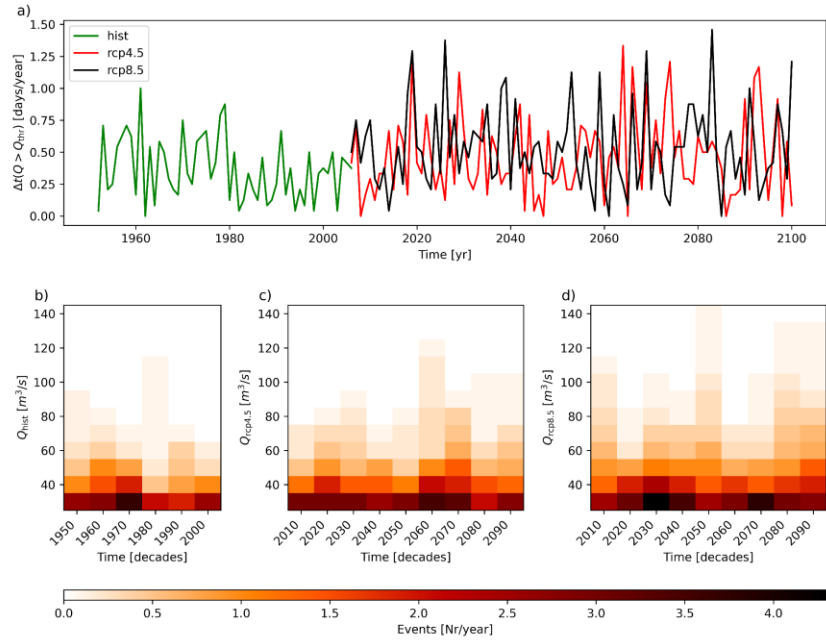


Fig S15 a) Cumulative duration of water discharge above the 99.9 % -ile in days per year for HIST (green line), RCP4.5 (red line), RCP8.5 (black line), for the city of Villanova. Number of events per year with peak values larger than specific values, grouped by decades for: HIST b), RCP4.5 c) and RCP8.5 d).

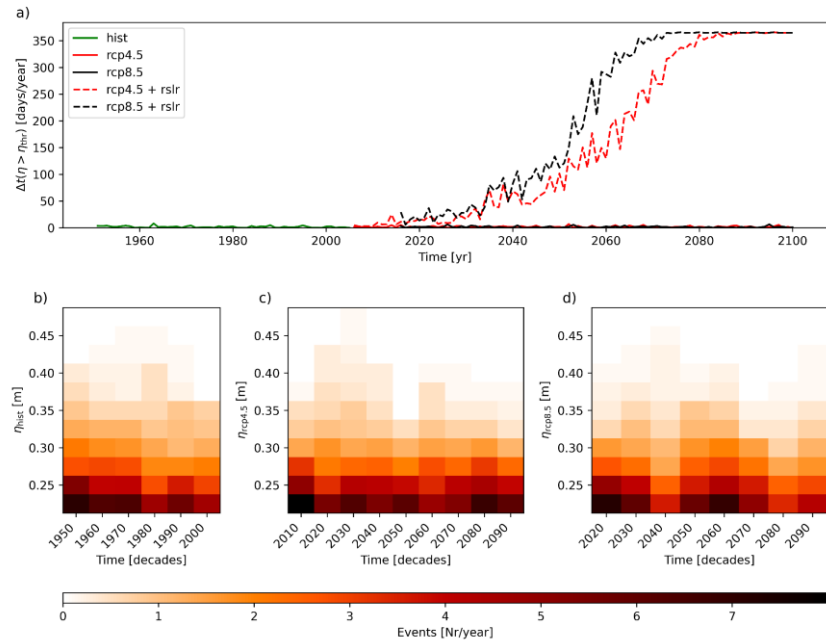


Fig S16 a) Cumulative duration of total water level above the 99.5 % -ile in days per year for HIST (green line), RCP4.5 (red line), RCP8.5 (black line), RCP4.5 and RCP8.5 plus the effect of RSLR (red dashed line and black dashed line, respectively), for the city of Oarsoladea. Number of events per year with peak values larger than specific values, grouped by decades for: HIST b), RCP4.5 c) and RCP8.5 d)

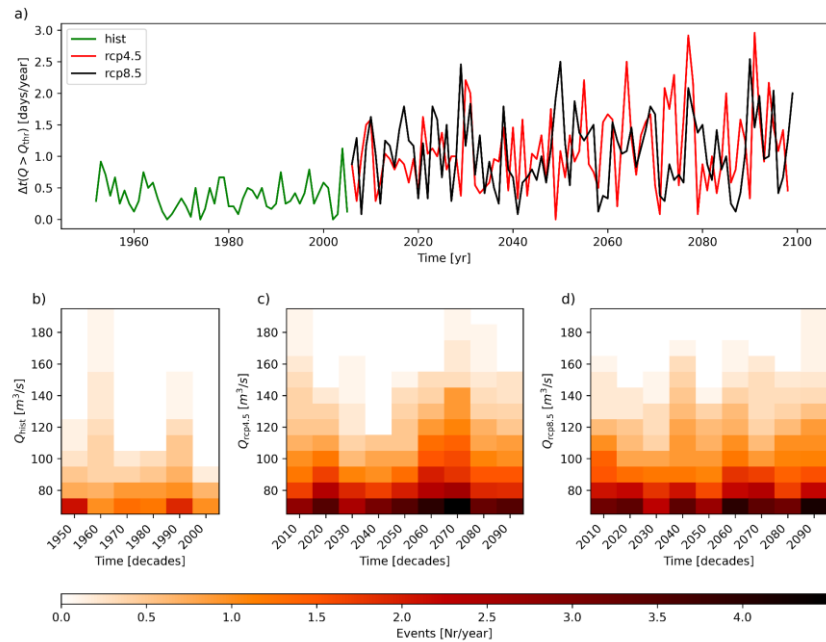


Fig S17 a) Cumulative duration of water discharge above the 99.9 % -ile in days per year for HIST (green line), RCP4.5 (red line), RCP8.5 (black line), for the city of Oarsoaldea. Number of events per year with peak values larger than specific values, grouped by decades for: HIST b), RCP4.5 c) and RCP8.5 d).

References

Dottori, F., Alfieri, L., Bianchi, A., Skoien, J., and Salamon, P.: A new dataset of river flood hazard maps for Europe and the Mediterranean Basin, *Earth Syst. Sci. Data*, 14, 1549–1569, <https://doi.org/10.5194/essd-14-1549-2022>, 2022.

Hersbach, H., Bell, B., Berrisford, P., Hirahara, S., Horányi, A., Muñoz-Sabater, J., Nicolas, J., Radu, R., Schepers, D., Simmons, A., Soci, C., Abdalla, S., Abellán, X., Balsamo, G., Bechtold, P., Biavati, G., Bidlot, J., Bonavita, M., Chiara, G., Dahlgren, P., Dee, D., Diamantakis, M., Dragani, R., Flemming, J., Forbes, R., Fuentes, M., Geer, A., Haimberger, L., Healy, S., Hogan, R. J., Hólm, E., Janisková, M., Keeley, S., Laloyaux, P., Lopez, P., Lupo, C., Radnoti, G., de Rosnay, P., Rozum, I., Vamborg, F., Villaume, S., and Thépaut, J.-N.: The ERA5 global reanalysis, *Q. J. R. Meteorol. Soc.*, 146, 1999–2049, <https://doi.org/10.1002/qj.3803>, 2020.

Muñoz-Sabater, J.: ERA5-Land hourly data from 1950 to present, Copernicus Climate Change Service (C3S) Climate Data Store (CDS), [data set] <https://doi.org/10.24381/cds.e2161bac>, 2019.

Vannucchi, V., Taddei, S., Capecci, V., Bendoni, M., and Brandini, C.: Dynamical Downscaling of ERA5 Data on the North-Western Mediterranean Sea: From Atmosphere to High-Resolution Coastal Wave Climate, *J. Mar. Sci. Eng.*, 9, 208, <https://doi.org/10.3390/jmse9020208>, 2021.

Ziese, M., Garcia, R., Dottori, F., Salamon, P., and Schweim, C.: EFAS upgrade for the extended model domain – Technical documentation, Publications Office, <https://doi.org/10.2760/806324>, 2019.